Coupling Between Homogeneous Rate Processes and Fluid Deformation Rate: Brownian Particle Coagulation in a Rapidly Dilating Solvent

Daniel E. Rosner
High Temperature Chemical Reaction Engineering Laboratory and Yale Center for Combustion Studies, Dept. of Chemical Engineering, Yale University, New Haven, CT 06520

Manuel Arias-Zugasti
Departamento de Física Matemática y de Fluidos, Facultad de Ciencias UNED, 28080 Madrid, Spain

DOI 10.1002/aic.12277
Published online May 18, 2010 in Wiley Online Library (wileyonlinelibrary.com).

P. Curie's principle applied to an isotropic medium of arbitrary EOS does not preclude coupling between homogeneous (chemical,…) rate processes and local fluid dilation rate. Yet, practical examples of this coupling have largely remained unexplored. Using recently studied supercritical "antisolvent" (SAS) examples for precipitating high-value particles (e.g., pharmaceuticals), we suggest that the characteristic dilation time t_V *of the swelling solvent can be small enough to noticeably reduce the operative coagulation rate "constant," β. Moreover, we expect that this coupling can occur under conditions in which postnucleation Brownian coagulation must be accounted for in predicting the efficacy of such micron-sized powder production methods. Accordingly, a rational approximate theory for this rate constant "correction factor," β/β(0), is proposed here, emphasizing the applicable limit of continuum Brownian diffusion control. We also present a preliminary assessment of the particle size distribution (PSD) consequences of these "corrections," implying strategies to reduce both mean particle size and PSD spread. Possible generalizations are indicated.* *AIChE J,* 57: 307–318, 2011
Keywords: supercritical antisolvent precipitation, P. Curie's coupling principle, precipitation from gas-expanded solvents, diffusion-controlled rate processes in solution, Brownian coagulation rate constant, quadrature method of moments (QMOM), orthogonal collocation

Introduction, Background

From the vantage point of linear irreversible thermodynamics, P. Curie's "admissible coupling" principle[1] applied to an isotropic medium of arbitrary equation of state does not preclude a "coupling" between a homogeneous (chemical,…) rate process and the local fluid dilation rate (the frame-invariant (scalar):[1–3] trace(def **v**) = div **v**). Yet, examples of this type of coupling have largely remained unexplored to this day,* and this particular "allowable" coupling is not even mentioned, no less accounted for, in essentially

Correspondence concerning this article should be addressed to D. E. Rosner at daniel.rosner@yale.edu.

*In the 1954 treatise of Hirschfelder et al.[4] one finds (p. 710) the sentence: "Such an effect has not been studied experimentally and is not further discussed here." As recently as 2007, Prof. R. B. Bird[5] has written (p. 767) that "we omit any further consideration of it" (this type of coupling) because of a perceived lack of experimental studies or realizations.

all recent studies of reaction rates occurring in variable density flows.

However, we propose here that the emerging field of supercritical fluid (SCF) process engineering[6] (see, e.g., the section on Recent Developments in "Supercritical Fluid Particle Processing," below)—in particular, particle precipitation/coagulation resulting from the use of a "supercritical antisolvent" (SAS) (to produce the supersaturations required for particle nucleation and growth)—already provides practical examples where this type of coupling will have to be accounted for to predict precipitated particle size distributions (PSDs). As discussed briefly in the following section (below), we expect that this coupling occurs under conditions in which postnucleation Brownian coagulation occurs in the "rapidly swelling" solvent. Although not yet studied in adequate detail, it already seems clear that this effect will have to be accounted for to predict the evolution of precipitate particle populations, and, hence, the efficacy of such micron-sized high-value powder production methods—especially when small (ca. sub-10 micrometer) solvent diameter sprays can be used at pressures well below the S/AS mixture critical point. Indeed, our work appears to provide incentives to deliberately work under such conditions to approach a desired degree of powder "monodispersity." Motivated by such emerging applications, a rational yet tractable approximate theory for the magnitude of this rate constant "correction factor," $\beta/\beta(0)$, is proposed and illustrated here—with emphasis on the applicable limit (for SCF-processing applications) of continuum Brownian diffusion-controlled coagulation, and its anticipated consequences for the narrowness of crystal size distributions (CSDs) resulting from Brownian coagulation in these remarkable processing environments. However, for completeness, we also briefly consider below the opposite conceptual extreme of rapid compression (negative dilation) and the expected net effects of alternating dilation and compression—in each case, deliberately suppressing (supplementary) thermal effects. We conclude with comments on the interaction of physically distinct coagulation mechanisms, including the intrinsic "nonadditivity" of β_{app} and the "nonfactorability" of the appropriate correction factors. Of necessity, each of these corollary topics will have to be revisited in greater detail in future work (see section on Recent Developments in "Supercritical Fluid Particle Processing"; General Case of a CSD).

Recent Developments in "Supercritical Fluid Particle Processing"

Many high-value fine powders of interest as pharmaceuticals (antibiotics, hormones,…), catalyst precursors, or energetic materials (RDX,…) can be produced under rather mild thermal or mechanical processing conditions by first dissolving these materials (perhaps originally synthesized in a coarse but biologically active form) into a suitable solvent and then inducing rapid nucleation and precipitation by simply spraying the liquid solvent into a suitable "SAS"—often high-pressure CO_2[7–13] A remarkable feature of this processing method, often abbreviated "SASP," is the volumetric expansion rate of the solvent when confronted with the SAS—a rate usually controlled by the rate of Fickian diffusion of the antisolvent vapor, e.g., CO_2, into the swelling solvent. This mechanism is associated with a characteristic dilation time—e.g., that interval associated with an e-folding of the mixture-specific volume, to scale as d_0^2/D— i.e., quadratically with the initial solvent droplet diameter. Now, most SASP experiments and associated modeling studies to date have assumed rather large initial solvent droplets—of the order of 50–100 μm diameter—for which the characteristic times governing the dilation process have been found to be of the order of hundreds of milliseconds. However, this implies that droplets smaller than about 10 μm in diameter—a range accessible by several advanced types of "atomizers"—would experience characteristic dilation times of the order of only tenths of milliseconds—values shown below to be short enough to actually influence coagulation rate "constants" for intermediate (but submicron) size particles growing as a result of their Brownian motion in these unusual processing environments. Moreover, because this rate of dilation, in effect, will preferentially "penalize" particles that become large, we would also expect a characteristic narrowing of the PSDs describing such particle populations—probably a desirable consequence of this previously unappreciated "coupling" (See section on Formulation of Diffusion-Controlled Coagulation with Dilation or Compression).

Based on our review of this recent "SASP" literature, as of this date only partial modeling steps appear to have been taken—often confined to suggesting rational estimates of additional characteristic times (associated with liquid jet break up, the nucleation time based on the growth of intradroplet supersaturation, etc.[14]). Significantly, we are not aware of any attempts to carry out a proper population balance on the particles precipitated in this admittedly complex (transient, dilating) N/G/C environment with spatially nonuniform local supersaturation. Accordingly, this article describes our initial steps[†] in this direction—steps expected to be necessary to ultimately enable the design, scale up, and optimization of such "SASP" processes in the future.

As briefly discussed in the discussion section (see subsection on Brownian Coagulation under "RESS" Conditions), the dilation rate effects considered here may also be relevant to the somewhat simpler (but perhaps less versatile) process called "RESS"— i.e., fine particle precipitation due to the rapid expansion of a supercritical solvent. In any case, our basic formulation (following section) is deliberately not process-specific, leaving open possible future applications to all types of SCF precipitation processes.

Analysis of Continuum Regime Brownian Coagulation in a "Dilating" Solvent: Theoretical Approach and Preliminary Expectations

Consider the following QS-diffusion-controlled coagulation rate calculation developed below to provide a universal "blowing"-type correction factor to the familiar "base case" Smoluchowski (continuum-limit) coagulation rate constant:

[†]In early 1997, one of us (DER) communicated to Prof. Debenedetti (Princeton/ChE) the idea that the coagulation rate constant in the SASP environment might be influenced by the antisolvent-induced dilation rate of the solvent. However, this notion was not pursued at that time—when there seemed to be more urgent research tasks associated with the use of SAS to "micronize" deliverable drugs without appreciable loss of biological activity (e.g., insulin dissolved in DMSO).

$$\beta_{12} = 4\pi(D_1 + D_2)(a_1 + a_2). \quad (1)$$

Here, the D_i are the (Einstein-Stokes) diffusion coefficients for the spherical particles of radii a_i in the prevailing continuum.

Before returning to the most general case, it will be instructive to first address the "quasi-monodispersed" case in which all of the participating particles are nearly of the same size. Thus, setting $a_1 = a_2 = a$ leads to the following size-independent reference value of β:

$$\beta_{\text{ref}} = \frac{8k_B T}{3\mu_S}, \quad (2)$$

where μ_S is the Newtonian viscosity of the carrier fluid (solvent). It is interesting to note that this "physical rate constant" has the units: m^3/s—or "volume flow rate."

Now consider a test solid particle of radius $a = d_p/2$ immersed in a fluid which is expanding (specific volume increasing) with the characteristic expansion time t_V, defined by the *e*-folding time[‡]:

$$t_V = (\text{trace}(\text{def}\,\mathbf{v}))^{-1} = (\text{div}\,\mathbf{v})^{-1}. \quad (3)$$

From the vantage point of an observer centered in this particle, there is a radial velocity field, which can be described by:

$$\text{v} = \frac{r}{3t_V}. \quad (4)$$

This radial velocity has the value $v_w = d_p/(6t_V)$ when evaluated at $r = a$. For the case of ordinary diffusion toward such a target, we expect the effect of such an outflow to depend on a Peclet number of the form:

$$Pe_w = \frac{\text{convective velocity}}{\text{diffusion velocity}} = \frac{v_w}{D/a}. \quad (5)$$

This viewpoint leads us to expect that the principal dimensionless parameter quantifying the reduction in the coagulation rate constant beta will be:

$$Pe_w = \frac{d_p^2/D}{12t_V}. \quad (6)$$

Introducing the Einstein-Stokes equation for the diffusivity D and the aforementioned β_{ref}, this parameter can also be written:

$$Pe_w = \frac{2\pi d_p^3}{3\beta_{\text{ref}} t_V} = \frac{4v_p/t_V}{\beta_{\text{ref}}}. \quad (7)$$

revealing that for a given characteristic time t_V, the effects of this "pseudoblowing" (see below) will increase rapidly with the diameter of the coagulating particles.

We show below that because of the formally unbounded radial velocity far from the target particle (cf. Eq. 4) it is also necessary to specify a physically relevant outer radius at which to impose the BC of known far-field composition for the collision partner. As will be seen, this introduces a so-called "cutoff radius," R_∞, i.e., a second parameter dependent on the prevailing particle volume fraction.

Summarizing, in a "dilational" situation such as that experienced in SASP applications we expect to be able to write:

$$\beta(Pe_w, \phi) = \beta(0) \cdot F(Pe_w, \phi), \quad (8)$$

where $\beta(0)$ is the "unperturbed" Smoluchowski coagulation rate coefficient, and the indicated function $F(Pe_w,\phi)$ remains to be calculated (see below) in a manner not unlike the classical blowing factor of mass/heat transfer theory (e.g., Eqs. 5.4–32 of Ref. 3):

$$F_b(Pe_w) = \frac{Pe_w}{e^{Pe_w} - 1}. \quad (9)$$

Recall that this familiar result is explicitly applicable to the case that the radial velocity *falls off* as the inverse square of the radius (cf. Eq. 4). However, as is also now known, this simple explicit law also applies to the modification in the coagulation rate constant associated with long-range Coulomb repulsion (or attraction)[15,16] (see, e.g., discussion section below) or even thermal forces associated with the Brownian coagulation of pairs of particles of unequal temperature.[17]

Calculating the relevant "dilation-rate" correction to the Smoluchowski rate constant

By imposing the outer boundary condition at a physically plausible radius fixed by the prevailing particle volume fraction, it is possible to solve the second-order linear ODE governing isothermal convective-diffusion of a dilute solute to obtain the ratio of the diffusion-controlled flux at $r = a = d_p/2$ when Pe_w is finite to its value when $Pe_w = 0$. Indeed, it is interesting to compare the result for the present case with the already familiar Eq. 9. Dilation rate-induced reductions in the Brownian coagulation rate constant are expected to be much more severe for a given Pe_w because of the increasing countercurrent "far" from the target. This expectation will be borne out in the section on Formulation of Diffusion-Controlled Coagulation with Dilation or Compression, where we report the results of appropriate numerical simulations.

In the following section, we first derive/solve the ODE satisfied by the normalized solute mass faction ω/ω_∞ and calculate the aforementioned function $F(Pe_w,\phi)$. This function is then displayed "once and for all" for use in future coagulation rate calculations and then generalized to embrace the more general case of Brownian coagulation of a polydispersed population of particles.

"Suction" augmentation of coagulation rate constant for "negative dilation"

When the radial carrier fluid velocity v changes sign we have the analog of the "suction" augmentation of diffusion flux to the centrally located "target" sphere. Indeed, despite our motivation to quantify dilation-rate effects in the SASP

[‡]Time interval in which the specific volume of the host vapor increases by a factor of *e*.

environment, it is of conceptual interest to also calculate/plot the corresponding values of $F(Pe_w,\phi) > 1$ for the case of "negative dilation rate"—corresponding to an isothermal compression. This function will also be displayed "once and for all" for use in future coagulation rate calculations and then generalized to embrace the more general case of Brownian coagulation of a polydispersed population of particles.

Net effect of alternating dilation and compression

By analogy with the case of "real" suction and blowing, we finally consider a situation in which the governing parameter $Pe_w = 4v_p/(t_V \beta_{ref})$ is not small and oscillates around zero because one repetitively goes from "dilation" ($t_V > 0$) to "compression" ($t_V < 0$). However, the highly nonlinear function $F(Pe_w,\phi)$ and $F(-Pe_w,\phi)$ are not equally far from unity. This leads us to expect that when dilation (pseudo-blowing) occurs the reduction in coagulation rate constant will not be as large as the increase that occurs in the compression (pseudo-suction) part of the cycle. On this basis, we expect that a sufficiently high-frequency "standing" sound wave should cause a net increase in the rate of Brownian coagulation rate of suspended dust particles—quite irrespective of temperature effects or particle "dynamical" response. These expectations are borne out in the following section, which contains the results of such coagulation rate simulations.

Formulation of Diffusion-Controlled Coagulation with Dilation or Compression

The evolution of a population of particles subject to Brownian coagulation in an expanding (or compressing) carrier fluid is described by the usual general dynamic equation (GDE)[16]

$$\frac{\partial n}{\partial t} = \mathcal{B} - \mathcal{D} - \frac{n}{t_V}, \tag{10}$$

where the particle production ($\mathcal{B}$) and destruction ($\mathcal{D}$) terms by coagulation are given by

$$\mathcal{B}(v) = \frac{1}{2}\int_0^\infty dv' \beta(v', v - v')\, n(v')\, n(v - v')$$
$$\mathcal{D}(v) = n(v) \int_0^\infty dv'\, \beta(v, v')\, n(v'), \tag{11}$$

where the coagulation rate constant β appears as a "kernel" in this integrodifferential equation. The additional term $-n/t_V$ is due to the change in number density n as a consequence of the expansion of the carrier fluid. Here, $|t_V|$ is the characteristic time defined by density variations ($t_V = (D \ln \rho^{-1}/Dt)^{-1}$), and positive (negative) values correspond to expansion (respectively compression) of the carrier fluid. This extra term is responsible for the time variation of the volume fraction occupied by the particles

$$\phi = \phi_0\, e^{-t/t_V}, \tag{12}$$

which is constant in the case of no carrier fluid specific volume change ($t_V \to \infty$).

As a consequence of the overall velocity drift produced by the expansion of the carrier fluid, the coagulation rate constant β is modified. As is customary, the coagulation rate in a density-varying environment can be computed as the long-time behavior of the flow rate of particles toward a target particle, corrected to take into account the movement of the target particle. In the continuum limit, the calculation of this flow rate is given by the solution of the convection-diffusion equation (Eq. 13) in terms of the mass fraction of particles (ω), with the effect of homogeneous density variations described by an isotropic "pseudo-blowing" flow velocity with a radial velocity given by Eq. 4, centered on the target particle.

Rather than computing a new coagulation kernel, the effect of density variations can be described with the usual coagulation kernel introducing a correction factor (F), computed as the ratio of particle flow toward the target particle in the expanding (or compressing) environment, over the corresponding flow found when the density is constant ($t_V = \infty$). To calculate that flow rate ratio, we compute the solution of the stationary convection diffusion equation

$$\frac{r}{3t_V} \cdot \frac{\partial \omega}{\partial r} = (D_1 + D_2)\frac{1}{r^2} \cdot \frac{\partial}{\partial r}\left(r^2 \frac{\partial \omega}{\partial r}\right) \tag{13}$$

with boundary conditions

$$\omega(r = a_1 + a_2) = 0, \quad \omega(r = R_\infty) = 1, \tag{14}$$

where a_i are the radii of the colliding particles, and R_∞ is the radius at which the concentration of particles reaches its outer, constant, far-field value. The necessity of introducing a finite value for the position R_∞ is a subtle question that does not arise in the calculation of the correction factor introduced in the coagulation rate by other processes, such as interparticle force fields, external force fields, or shear.[15,16] In those cases, the volume fraction occupied by the particles is constant, and the stationary solution of the transport equation that determines the coagulation rate gives a well-defined finite value of β. However, as a consequence of the formally unbounded radial velocity far from the target particle (Eq. 4), the long-time behavior of this equation leads to a zero coagulation rate in the case of dilation, which is a consequence of the limit behavior ($\phi \to 0$) found at long times if $t_V > 0$. A possible way to avoid this problem is to consider that the Brownian coagulation rate in an expanding environment depends on the volume fraction ϕ. This dependence enters the model by estimating the R_∞ parameter corresponding to particles with radii a_1 and a_2 as the sum of the radii of the "average void regions" surrounding these particles, computed in terms of ϕ:

$$R_\infty = (a_1 + a_2)\phi^{-1/3}. \tag{15}$$

Thus, the process of coagulation under time-independent density variations is described here as a quasi-steady process, which depends on time through the volume fraction of the particles (ϕ), according to Eq. 15. Although the introduction of this additional parameter seems a physically reasonable way of describing the time dependence of coagulation in compressible environments, it is clear that this proposed estimation of R_∞ as a function of the volume fraction is not the only possibility.

Solving the ODE equation (Eq. 13) with the aforementioned BC Eq. 14), the modified coagulation rate $\beta(Pe_w,\phi)$ is found, and the correction factor $F(Pe_w,\phi)$ is then defined as the ratio between the coagulation rates with and without the modification produced by the rate of carrier fluid specific volume change

$$F(Pe_w,\phi) \equiv \frac{\beta(Pe_w,\phi)}{\beta(Pe_w=0,\phi_0)}. \quad (16)$$

Hence, we find that the correction factor is given by

$$F(Pe_w,\phi) = \left(1-\phi_0^{1/3}\right) \Big/ \left[1-\phi^{1/3}e^{Pe_w\left(\phi^{-2/3}-1\right)} + e^{-Pe_w}\sqrt{\pi Pe_w}\left(\mathrm{erfi}[\phi^{-1/3}\sqrt{Pe_w}]-\mathrm{erfi}[\sqrt{Pe_w}]\right)\right], \quad (17)$$

where the Peclet number corresponding to particles with radii a_i and a_j is

$$Pe_w = Pe_{w,ref}\cdot\frac{a_i a_j}{a^2}\cdot\frac{a_i+a_j}{2a}, \quad (18)$$

where a is the reference particle radius, and where the reference Peclet number ($Pe_{w,ref}$) is given by Eq. 7 with $d_p = 2a$. As can be seen, the Peclet number that enters the coagulation rate of particles of different sizes (Eq. 18) is given by Eq. 5, but with the convective and diffusion velocities evaluated at $a_i + a_j$, and with the diffusion coefficient corrected to take into account the relative motion.

On the other hand, as a consequence of the former result (Eq. 17), the asymptotic value reached by the correction factor $F(Pe_w,\phi)$ in the limit of low volume fraction in the dilation case ($Pe_w > 0$) is simply $F(Pe_w,\phi= 0) = 0$, and in the compression case ($Pe_w < 0$)

$$F(Pe_w,\phi=0) = \frac{1}{1-e^{|Pe_w|}\sqrt{\pi|Pe_w|}\,\mathrm{erfc}\left[\sqrt{|Pe_w|}\right]}. \quad (19)$$

Finally, the correction factor $F(Pe_w,\phi)$ (Eq. 17) is shown as a function of the Peclet number for several values of ϕ on Figure 1.

'Quasi-monodispersed' case

In the monodisperse case, the radii of the particles are given by $a_i = a(t)$, and the reference particle radius is given by the initial radius $a = a_0$. Hence, the dependence of the correction factor on particle size (given by Eq. 18) reduces in this case to

$$Pe_w = Pe_{w,ref}\cdot\left(\frac{a(t)}{a_0}\right)^3. \quad (20)$$

Thus, the impact of the rate of expansion of the carrier fluid in the coagulation rate is much higher as larger particles are considered. As a consequence, in the case of an expanding carrier fluid, the coagulation rate decreases very fast as larger particles are considered, introducing an effective limit to the particle size that can be reached by coagulation. On the other hand, if the carrier fluid is compressing, the coagulation rate is enhanced with a correction factor that increases with particle size, hence favoring the formation of larger particles.

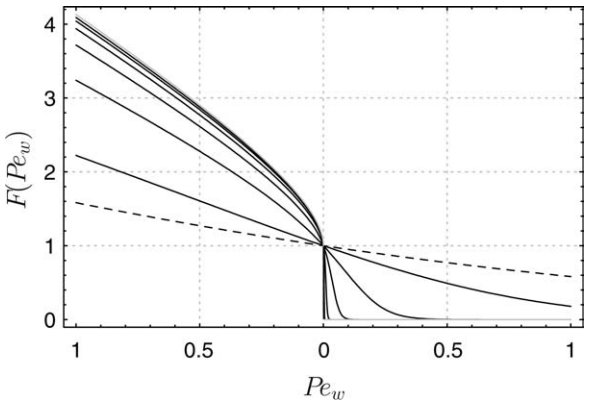

Figure 1. Coagulation rate constant correction factor $F(Pe_w,\phi) \equiv \beta/\beta(0)$ as a function of the Peclet number Pe_w for volume fractions ϕ between 10^{-6} and 10^{-1} in steps of 10^{-1} (solid lines), together with the asymptote reached at ϕ = 0 (thick gray line).

The familiar "blowing" correction factor $Pe_w/(e^{Pe_w}-1)$ is also shown for comparison (dashed line). Positive values of Pe_w correspond to dilation and negative values to compression.

As a consequence, the effect of carrier fluid expansion on the population polydispersity is reversed depending on whether the carrier fluid is expanding or compressing. If the carrier fluid is expanding and the initial population is almost monodisperse, then it will remain very close to a monodisperse population during the process of coagulation. On the other hand, if the carrier fluid is under compression, then the population will not be able to remain close to a monodisperse population.

The following figures (Figures 2 and 3) show the time evolution of a monodisperse population of particles for several initial volume fractions and several Damköhler numbers (defined as the ratio of expansion to coagulation times $Dam \equiv t_V/t_\beta$). The results have been formally computed for both cases: dilation and compression. In the case of compression, the calculations are computed from $t = 0$ until the theoretical maximum value of the volume fraction of the particles is reached (about 0.634 for random close packing in the monodisperse case).

On Figure 2 the evolution of the number density is shown and a small but noticeable difference can be seen between the results computed without the correction factor introduced by the expansion rate of the carrier fluid (i.e., assuming $F = 1$) and the corresponding results including this correction factor. This difference becomes more appreciable in the results for the particle size, shown in Figure 3.

General case of a CSD

In the case of a polydisperse population, the former qualitative conclusions related to the evolution of the polydispersity of the population still apply.

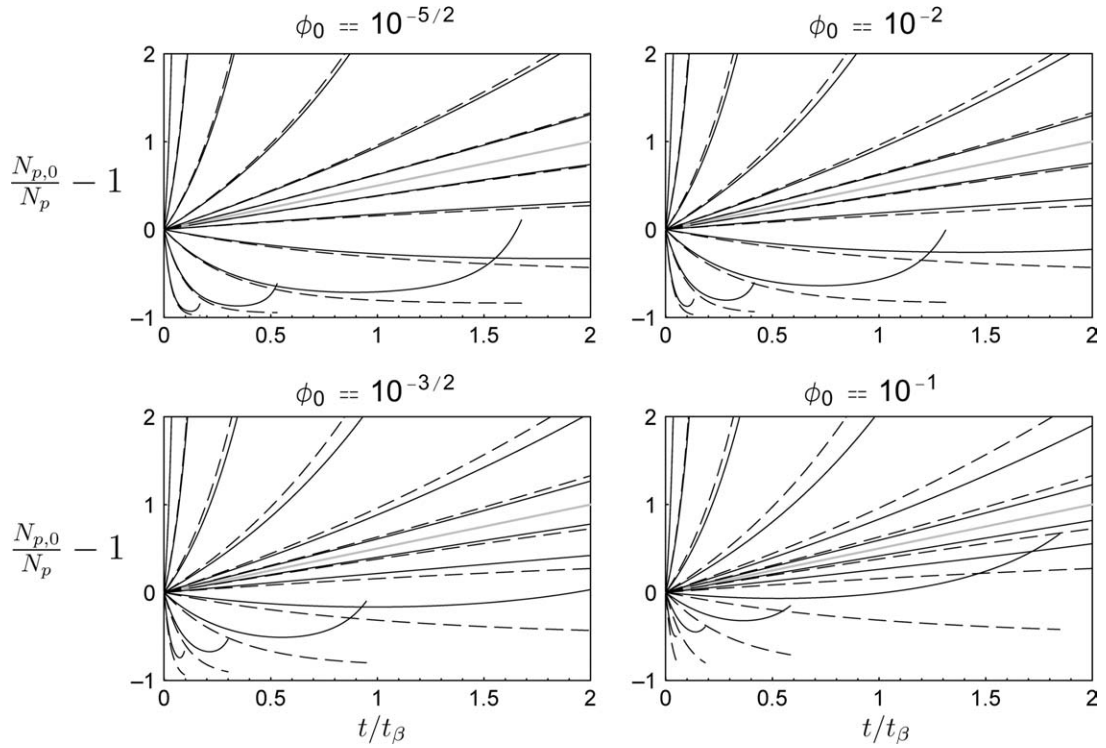

Figure 2. Inverse number density ratio $N_{p,0}/N_p - 1$ vs. t/t_β in the monodisperse case for Damköhler numbers between $10^{-3/2}$ and 10^{1} in steps of $10^{1/2}$ and for several values of the initial volume fraction ϕ_0.

The solid lines correspond to results including the correction factor F (Eq. 17), and the dashed lines to results assuming $F = 1$. The thick gray line corresponds to results without carrier fluid specific volume change. The lines above (below) the thick gray line correspond to dilation (respectively compression).

In the case of coagulation in an expanding environment, the coagulation process is limited to a time interval (of order t_V) before the volume fraction of particles becomes negligible. During that interval the average particle size and the standard deviation of the population will increase, but as a consequence of the strong penalty imposed by the expansion rate of the carrier fluid on the coagulation rate of the larger particles, the average particle size and the standard deviation of the population will be smaller than their respective expected values computed without taking into account the effect of the carrier fluid rate of expansion.

On the other hand, in the case of coagulation in a compressing environment, the coagulation process can only take place until the upper limit of the volume fraction of the particles is reached (0.634 for random packing in the monodisperse case; higher values, but always below 1, can be reached in the polydisperse case), which will also happen in a time interval of order t_V. During that period the average particle size and standard deviation of the population will increase faster than the corresponding expected result computed without taking into account the effect of the carrier fluid rate of (in this case negative) expansion.

Illustrative numerical results for attainable conditions of Pe_w and ϕ (SASP)

The results shown in this section correspond to the evolution of a polydisperse particle population, in an expanding environment, with nominal values of Damköhler number and initial volume fraction relevant to the SASP process. i.e.: $Dam = 1/10$ and $\phi_0 = 1/100$.

The initial condition for the distribution of sizes considered here is

$$f(x) = ax^2 e^{-bx}, \tag{21}$$

where x is the dimensionless particle volume $x = v/v_{ref}$, with the reference volume (v_{ref}) defined as the volume corresponding to the Sauter mean diameter (SMD). In the former Eq. 21 a is determined by the normalization condition, and b is determined by the condition that the dimensionless volume of a particle with the SMD is $x = 1$. Besides this initial condition, a significant amount of computations was performed considering other initial distributions. In all the cases, the qualitative results were the same.

The time evolution of the aforementioned initial distribution has been computed in terms of QMOM, which gives information about the lowest order moments of the distribution, and orthogonal collocation, which computes the evolution of the distribution as a continuous function. None of the two mathematical methods considered relies on presumptions about the mathematical form of the PDF.

Results from QMOM. The time evolution computed using QMOM[18,19] shows that, under the conditions considered, the coagulation rate becomes negligible at $t/t_\beta \simeq 0.5$. During the limited time in which the coagulation process is still important, the mean particle volume increases slightly,

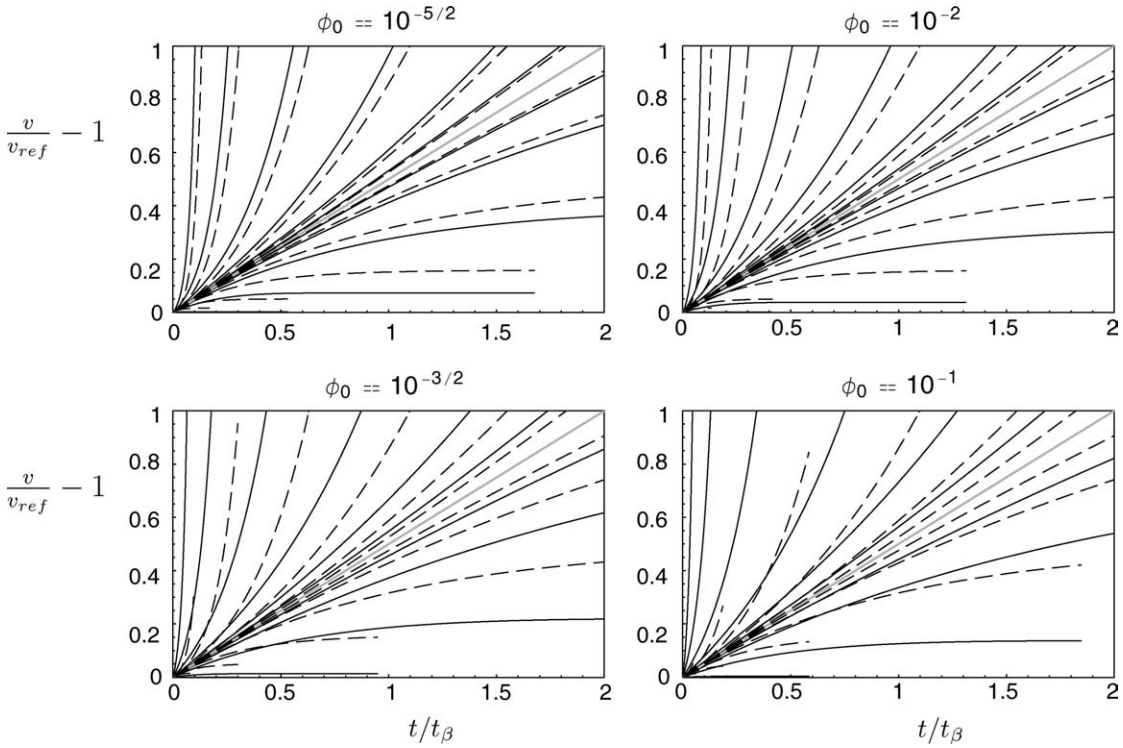

Figure 3. Time evolution of particle size in the monodisperse case for Damköhler numbers between $10^{-3/2}$ and 10^{1} in steps of $10^{1/2}$ and for several values of the initial volume fraction ϕ_0.

The solid lines correspond to results including the correction factor F (Eq. 17), and the dashed lines to results assuming $F = 1$. The thick gray line corresponds to results without carrier fluid specific volume change. The lines below (above) the thick gray line correspond to dilation (respectively compression).

as well as the standard deviation of the population. After this period, the coagulation rate becomes completely negligible, and accordingly the number density distribution function decreases without changing its shape as the host fluid expands.

The results for the lowest order moments of the number density distribution function, including the effects owed to the expansion of the host fluid, differ strongly from the corresponding results in absence of expansion. The main reason for this is because in a continuously expanding environment the volume fraction of particles decreases exponentially with time. Besides the effect owed to the decrease in number density produced by the expansion of the host fluid, the modification introduced in the coagulation rate as a consequence of the host fluid expansion rate introduces an additional correction in the time evolution of the number density distribution function. The results found for $Dam = 1/10$ and $\phi_0 = 1/100$ show that this additional correction is modest but noticeable for the average particle size and standard deviation, becoming more important for the higher order moments of the distribution function, as for instance the skewness (symmetry) and kurtosis (degree of "peakedness") of the PDF (see Figure 4).

Results from Orthogonal Collocation. The time evolution of the initial distribution (Eq. 21) as a continuous function has been computed solving the GDE of the population (Eq. 10) by means of the spectral orthogonal collocation method.[20] The calculations shown here were performed using a spectral basis of 50 Whittaker cardinal functions (similar results were found using a basis of Laguerre functions). The coagulation term at the collocation abscissae was efficiently computed by means of the "fast algorithm".[21] To validate the present numerical method, the self-similar distribution function corresponding to a constant volume environment has also been computed solving the corresponding GDE (Eq. 10 with $t_V = \infty$) using orthogonal collocation with the coagulation term approximated by the "fast algorithm,"[21] and the results are shown in Figure 5 (gray line) together with the corresponding results computed by Vemury and Pratsinis[22] (for aggregate fractal dimension = 3) using a sectional method (solid dots).

The main conclusion that can be extracted from the present calculation, corresponding to the parameter values $Dam = 1/10$ and $\phi_0 = 1/100$, is that the self-similar distribution function reached in the case of an expanding environment is much narrower than the corresponding result found in absence of expansion. Besides this effect, there is also a small but noticeable difference between the self-similar distribution function computed with the corrected coagulation rate (Figure 5, solid line) and with the usual coagulation rate (Figure 5, dashed line).

Discussion

Principal consequences for dilating-, compressing- and oscillatory- particle-containing environments

As pointed out in the critical reviews/extensions of, say, Noyes,[23] Wilemski and Fixman,[24] Rice,[25] Szabo,[26] and Friedlander,[16] there have been many refinements of the

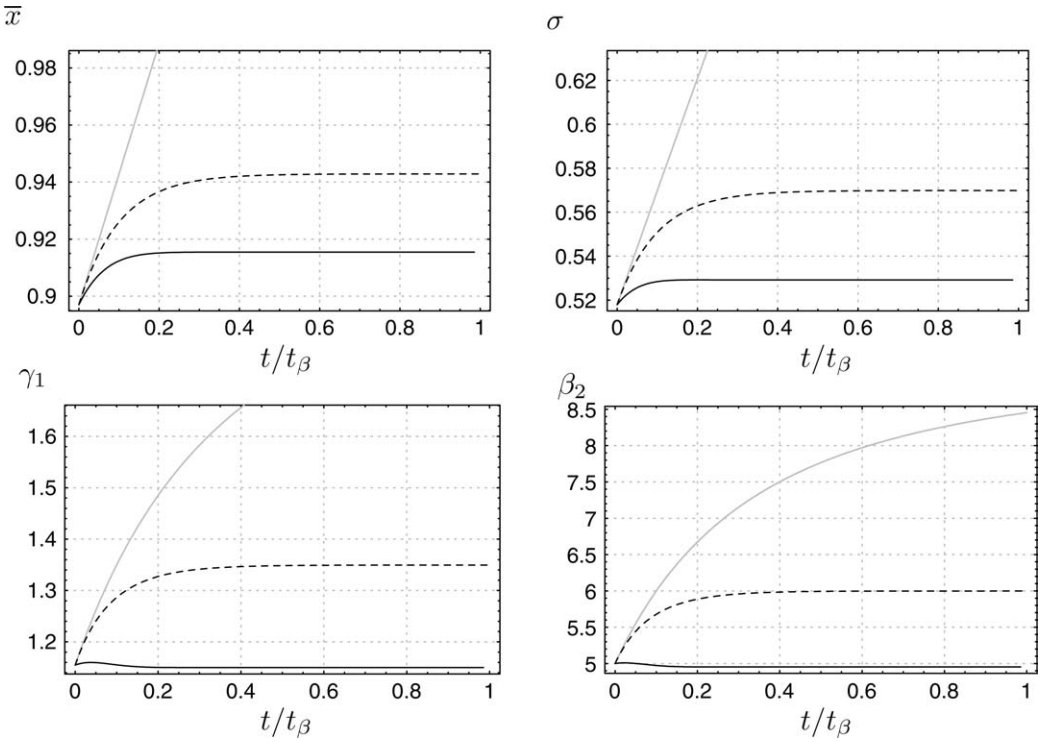

Figure 4. Time evolution of average mean size $\overline{x}$ (top left), PSD-standard deviation σ (top right), skewness γ_1 (bottom left), and kurtosis β_2 (bottom right).

The solid lines show results with the corrected coagulation rate, the dashed lines show results assuming $F = 1$, and the thick gray lines correspond to results without carrier fluid specific volume change.

seminal Smoluchowski formulation (1917) of diffusion-controlled reactions in three-dimensional continua (a formulation[§] usually cast in terms of a diffusion equation (with effective diffusivity $D_i + D_j$) for the time-dependent pair probability density $p_{ij}(r,t)$ in the vicinity of one of the spherical reagents (of radius a_i) placed at the origin of a spherical coordinate system, subject to the perfectly absorbing BC imposed at $r = a_i + a_j$). As our present purpose has been to initiate an examination of the previously unstudied consequences of solvent dilation rate, we have deliberately limited ourselves here to the simplest form of Smoluchowski rate theory. However, to successfully model coagulation dynamics in specific SASP systems of future interest, we anticipate the need to relax several, if not ultimately all, of these useful simplifications.

Finally, note that we have deliberately cast the present analysis in terms of the physical time, t_V, characterizing the relative rate of change of specific volume for a fluid parcel—i.e., a characteristic time which (invoking the fluid's EOS, $\rho^{-1} = V/M = (\mathcal{R}T/p) \cdot (Z/M)$), without any loss of generality, can be written:

$$t_V = \left(\frac{1}{Z}\frac{DZ}{Dt} + \frac{1}{T}\frac{DT}{Dt} - \frac{1}{p}\frac{Dp}{Dt} - \frac{1}{M}\frac{DM}{Dt} \right)^{-1}. \qquad (22)$$

Accordingly, t_V will generally receive contributions from changes in the mixture compressibility factor Z, as well as temperature T, mixture molecular weight M (via composition), and the pressure, p. It is true that in our recent constant pressure ideal gas counterflow diffusion flame studies[27]) the DT/Dt term dominated the others, but the associated characteristic time was still as large as 10 ms, i.e., not small enough to appreciably modify the "free-molecular" encounter rate of our embryonic Al_2O_3(c) nanoparticles (see,

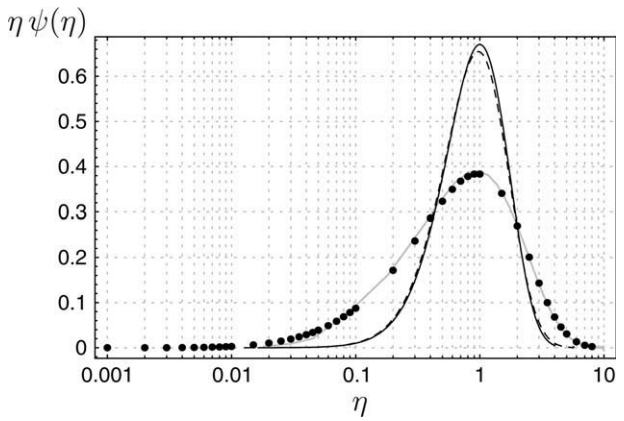

Figure 5. Normalized self-similar particle size distributions ψ vs. $\eta = x/\overline{x(t)}$.

The solid (dashed) lines correspond to PSD results including (respectively not including) the dilation correction factor F (with $Dam = 1/10$ and $\phi_0 = 1/100$). The thick gray line and the solid dots correspond to PSD results without carrier fluid specific volume change.

[§]Szabo[26] describes Smoluchowski's formulation as "The most familiar, but not necessarily the best understood"….

also, section on Brownian Particle Coagulation in the "Free-Molecule" Limit, below). In contrast, in our isobaric, near-isothermal "SASP" examples, the $Z(t)$ and $M(t)$ terms dominate and t_V can evidently be as small as 0.1 ms in a near-continuum local environment (on the scale of growing precipitate particles). It is this SASP confluence that can make the operative rate "constant" β_{ij} dilation-rate dependent.

It should not be assumed that our present analysis is limited to the (overly restrictive) case that t_V is actually a constant, because this important characteristic time, t_V (see Eq. 22 above), will generally be a (slowly varying-) function of the clock time t, and, perhaps only occasionally small compared with the characteristic coagulation time: $(\beta_0 N_{p,0})^{-1}$. On this basis, we envision that the present coagulation rate approach could be reasonably applied in quasi-steady fashion so long as $|dt_V/dt|$ is much smaller than $(16/3)|Pe_w|^{-1}$.

More familiar modifiers of the coagulation rate "constant"

Local correction factors to the classical Smoluchowski diffusion-controlled coagulation rate constant are not without precedent in aerosol science and technology.[16] Perhaps, most familiar are those associated with the superimposition of particle "drift"—due to either local electric fields[15] or thermal fields.[17]

Coulomb Repulsion or Attraction[15]. If participating particles i and j possess the number of elementary charges z_i and z_j then Coulomb forces produce either a "repulsive" or "attractive" drift velocity in a viscous medium. This leads to the now familiar correction factor:

$$z(x) = \frac{x}{e^x - 1}, \tag{23}$$

where:

$$x = \frac{z_i z_j e^2}{k_B T (a_i + a_j)}. \tag{24}$$

Interestingly enough, this factor is identical to the "blowing" correction governing the reduction in diffusion rate to a stationary target sphere emitting a steady mass flux at its surface.[3]

Thermal Forces for Unequal Particle Temperatures. Suspended particles with a temperature different from that of the local carrier gas are surrounded by nonuniform temperature fields, which can exert a net "thermal force" on nearby particles. Remarkably, Mackowski *et al.*[17] have shown that the aforementioned correction factor $x/(e^x - 1)$ also applies to this case provided one makes the identification:

$$x = \frac{(a_i + a_j) \cdot [F_T(a_i + a_j)]}{k_B T_g}, \tag{25}$$

where $F_T(a_i + a_j)$ is the effective net thermal force $(V_{T,i} + V_{T,j})/(B_i + B_j)$ evaluated at interparticle separation distance $a_i + a_j$. Here, $V_{T,i}$ and B_i are the QS thermal drift velocity and mobility of particle i, respectively, when particle i is exchanging energy with the surrounding gas at temperature T_g.

From this broader perspective, our present normalized correction factor $F(Pe_w, \phi)$ for carrier fluid dilation rate (Eq. 16 and Figure 1) will be seen to be of the same general type, but far more nonlinear than those previously introduced/studied. This fact will inevitably have important implications for: (a) numerical methods applied to the nonlinear population balance equation (section on Recent Developments in "Supercritical Fluid Particle Processing"; General Case of a CSD), (b) coagulating systems experiencing alternating dilation and compression, and (c) systems where several of these physically distinct mechanisms are operating simultaneously.

Coagulation in a Temperature Gradient. It has been clear for many years that particle size-dependent thermophoretic drift could be the cause of coagulation for particles of unequal size suspended in a fluid with a significant temperature gradient. Indeed, in the context of optical wave guide synthesis from doped silica suspensions in hydrogen gas combustion products, Rosner and Park[28] showed that this mechanism could not compete with ordinary Brownian coagulation even in the presence of temperature gradients (locally perpendicular to the deposit surface) of the order of ca. 10^5 K/m. But this was by no means a general conclusion, and we plan to develop the relevant theory further and investigate other engineering applications (e.g., involving higher pressures) in the near future. In this connection, it is also interesting to mention the relevant nonequilibrium thermodynamics work of Reguera and Rubi,[29,30] who explicitly considered the possible systematic effects of a temperature gradient (via the preferential loss of subcritical clusters) on the rate of homogenous nucleation of a locally supersaturated condensable vapor dilute in an otherwise quiescent carrier gas—an environment normally encountered in so-called "laminar diffusion cloud chamber" experiments.[31] Although this effect was found to be negligible under typical experimental conditions (e.g., pentanol vapor at p near 100 kPa), these authors speculated that such effects would become important for polymer crystallization applications.

Fluid "shear-induced coagulation" in the absence of Brownian motion

Ironically, Smoluchowski himself introduced an approximate coagulation rate constant which is explicitly "deformation-rate dependent." This is the equally familiar coagulation rate constant associated with finite-size, inertia-less suspended particles overtaking one another because of their unequal velocities in a laminar shear flow—often simply written[16]:

$$\beta_{ij} = \frac{4}{3}(a_i + a_j)^3 \left|\frac{\partial u}{\partial y}\right|. \tag{26}$$

We note that this interesting result, which has been adapted to predict time-averaged coagulation rates in turbulent flows, is rarely discussed from the TIP viewpoint of Curie's principle[¶]. Revisiting this particular formulation from our present perspective will be the subject of a future communication. In this connection, Reguera and Rubi also used their MNET formalism (mesoscopic nonequilibrium thermodynamics) to examine the possible effects of a shear flow on the rate process of homogeneous nucleation.[30]

[¶]Belfiori et al.[32,33] have recently raised this interesting issue in connection with the apparently stress-dependent biocatalytic activity of cells fixed to the walls of an empty tubular reactor. In contrast, our present emphasis is on "homogeneous" rate processes in an isotropic reacting medium "far" from macroscopic (intrinsically anisotropic) interfaces.

Although this effect was found to be negligible under typical laminar gas flow diffusion cloud chamber experiments, again polymer crystallization applications were suggested to be more likely candidates for appreciable effects of this type.

Treatment of "combined" effects

Of course, the aforementioned coagulation mechanisms need not occur in isolation, and we must anticipate environments in which various combinations will be operative. Although such combinations remain to be investigated, it is already clear that the extreme nonlinearity of the present dilation-rate correction factor $F(Pe_w, \phi)$ will probably preclude simple approximations such as "additivity of drift velocity" (to define an operative $Pe_{w;eff}$) or "factorability" of the individual correction factors. Of special interest in the SASP environment will be possible interactions between the effects of dilation rate and electrical charge.

Comment on "reciprocity"

In principle, "reciprocity" would suggest that the dilation rate-modified rate constant considered here should be related to a contribution to the effective bulk- (dilational) viscosity of such a mixture.[2] However, for the dilute solute-derived particle loadings of primary interest here, the consequences of this reciprocity are expected to be negligible.

Brownian particle coagulation in the "free-molecule" limit

In the more classical field of aerosol dynamics (e.g., low volume fraction nanoparticle dusts or mists in the atmosphere) fine particle coagulation often occurs in the so-called "free-molecule" regime in which the suspended particles can be treated as a hard-sphere pseudo-gaseous constituents in an ideal gas mixture.[16] As ideal gases (i.e., $Z = 1$) are notoriously "compressible," it is natural to inquire whether Brownian coagulation in this type of environment is also likely to lead to dilation rate modifications of the corresponding coagulation rate constant.

In such "nondiffusion-controlled" cases, the effective "blowing" (or recession-) velocity evaluated at the surface of a target particle must be compared with the mean thermal speed of the likely particle collision partners. This gas-kinetic theory line-of-reasoning leads to the expectation that the relevant Peclet number for assessing dilation-rate effects in the "free-molecule" coagulation limit will be of the "speed-ratio"** form:

$$Pe_{\mathrm{eff,fm}} = -S = \frac{d_p/a_g}{6t_V}\sqrt{\frac{\gamma_g m_p}{2m_g}}, \tag{27}$$

where a_g is the acoustic speed in the carrier gas, and γ_g is its specific heat ratio (a parameter near 1.27 for CO_2). Again, dilation-rate conditions would have to be such that the absolute value of this parameter $-S = \mathcal{O}(10^{-1})$ in an environment in which Brownian coagulation is itself important.

Steady gas expansions in a nozzle when the upstream plenum gas contains a condensable vapor constitute an interesting environment with a long history of study in the fields of steam turbine design and high-speed wind-tunnel testing. More recently, Turner et al.[35] carried out a theoretical study of the use of such a technique as a continuous source of nearly monodispersed droplets—with illustrative calculations for the case of N_2 carrier gas ultimately containing ca. 100-nm diameter droplets of the model organometallic compound: aluminum *sec*-butoxide (a precursor for alumina particle synthesis). Even though submillisecond dilation times t_V are achievable in this manner, when one computes the aforementioned parameter $Pe_{\mathrm{eff,fm}}$ one finds values near 2×10^{-4}, some 3—4 decades smaller than would be necessary for appreciable dilation rate effects on β_{fm}. Moreover, typical droplet volume fractions considered were in the range of only 20 ppm, again some 3 decades smaller than necessary for appreciable Brownian coagulation rate effects in this low residence time (ca. ms) environment. We conclude from this (and similar) example(s) that the coupling effect of principal concern in this article is not likely to be encountered in the so-called "free-molecule" regime. By way of sharp contrast, this class of coupling effects will probably not be "exceptional" in dealing with "SASP" environments.

Brownian coagulation under "RESS" conditions

If the SCF (e.g., CO_2) is itself used as the solvent and is simply isentropically expanded in a converging nozzle to achieve a transonic velocity, then the associated reduction in carrier fluid density will be accompanied by a loss of solvent power and, hence, precipitation. This alternative mode of fine particle production, reviewed by Tom and Debenedetti[36] and, more recently, by Jung and Perut[10] and Fages et al.,[11] exploits the RESS but is intrinsically limited by the lower solubility of many polar compounds in pure CO_2 (cf., the ordinary liquid solvents used in SASP). Nevertheless, it is of interest to briefly consider whether the dilation rate coupling we address in the preceeding section on Brownian particle coagulation in the "free-molecule" limit is likely to also play a role in modeling particle population evolution in RESS processing.

This important question deserves to be investigated more thoroughly on a case-by-case basis. However, it would appear that although the nozzle dilation rate conditions in RESS may be adequate to cause a noticeable local reduction in the operative coagulation rate constant for ca. 100-nm diameter particles (based on our estimate of the relevant parameter: Pe_w), the associated particle volume fractions (perhaps less than 100 ppm) are often too small for continuum-regime Brownian coagulation to be important in the available (ca. submillisecond) nozzle residence times (see, e.g., the idealized phenanthrene/CO_2 calculations of Kwauk and Debenedetti[37]). Depending on the choice of solute/solvent and operating conditions, the primary location for particle nucleation may actually be in the postnozzle or postcapillary "free-jet" expansion.[38,39] Turk[40,41] has called attention to the remarkable nucleation/coagulation environment in the supersonic "free-jet" immediately downstream of a RESS-capillary tube. In such a region dilation times and residence times are in the submicrosecond range, and predicted solute supersaturations become high enough ($>10^5$) to generate (via CNT) large numbers of particles in the "nanometer" (ca. 2–4 nm) diameter range—diameters comparable to the local CO_2 mean free path. Ironically, although the process of coagulation for such

**Indeed, in a one-dimensional (planar surface) system one might expect that $F(S)$ has the form: $F(S) = e^{-S^2} + \sqrt{\pi}S[1 + \mathrm{erf}(S)]$, where $S < 0$ for dilation (and vice versa) based on the suspended particle collision rate with a translating surface.[34] For S near 0 this behaves like $1 + \sqrt{\pi}S + S^2 + \ldots$.

small particles is likely to be important on this time scale, the associated dilation-rate–based Pe_w values appear to be marginal (i.e., smaller than 10^{-1}). Further work will be necessary to explore coagulation rates in the interesting free-jet region.

For completeness, we should also mention that a rather extreme example of suspended particle coagulation during recompression occurs in the RESS environment when nanoparticles nucleated in the aforementioned free-jet expansion (e.g., downstream of a capillary tube) ultimately encounter the so-called "Mach disk"— i.e., a strong locally normal shock wave which abruptly terminates the "overexpansion" process. Particle residence times and t_V values within this bulk viscosity thickened quasi-one-dimensional shock structure may be in the nanosecond range, and the inertia of even nanoparticles cannot be ignored in such a transient environment. Thus, although the formally calculated S-value may be adequate for noticeable enhancements in the coagulation rate constants, conditions within such nonisothermal gas dynamic structures will require a more general kinetic theory treatment than that sketched in the preceeding section.[42]

In summary, it seems clear that more realistic process models will be needed to fully exploit/optimize both RESS- and SAS-particle precipitation technologies.

Conclusions

In this work, we consider the coupling between Brownian particle coagulation in the continuum limit and rapid density variations in the host "vapor" (dilation/compression). It is shown that density variations in the carrier fluid produce a modification to the coagulation rate constant, which is positive for compressing vapors and negative for dilating vapors. In our theoretical model, we derive a closed form expression for the correction factor (F) to the coagulation rate constant, $F = \beta/\beta(0)$, which depends on the particle size through a Peclet number (Pe_w), defined as the ratio between the characteristic velocity introduced by the density variations of the host vapor, over the characteristic particle diffusion velocity. Although this type of "coupling" between a homogeneous (chemical,…) rate process and the local fluid dilation rate has been considered possible for a long time, to the best of our knowledge this is the first time that such coupling has been analyzed in detail.

The emergence of SCF processes for the production of high-value "micronized" powders appears to provide, perhaps for the first time, industrially significant examples of homogeneous rate processes (here submicron particle coagulation as the result of Brownian motion), which can be influenced in a fundamental way by the rates of fluid dilation. We suggest that this is especially true for the precipitation/evolution of fine particles as the result of spraying solute-containing small diameter liquid solvent droplets into a SAS—such as dense CO_2. We note that this type of "coupling" has long been considered possible, but has essentially remained unstudied for over 1 century. Our present approach for simulating these anticipated effects, and their interesting predicted consequences for emerging PSDs, has been outlined, illustrated, and briefly discussed in this initial article. Although further refinements are anticipated, we view this as a necessary first step on a path to ultimately providing a self-consistent framework to enable the design, scale-up and optimization of higher performance SCF-based precipitation processes in the future.

Acknowledgments

The authors gratefully acknowledge the support of NSF (via Yale Grant #CTS 0522944), Ministerio de Ciencia e Innovación (via UNED grant #ENE2008-06515-C04-03), and Comunidad de Madrid (via UNED grants #S-0505/ENE/0229 and #S2009/ENE-1597) as well as helpful discussions from their colleagues: Dr. Robert McGraw, Dr. Juan Fernandez de la Mora, Dr. Pedro Garcia-Ybarra, and Dr. Jose Castillo.

Notation

Symbol definition

a = particle radius
a_g = acoustic speed (of gas)
$\mathcal{B}$ = "birth" rate associated to particle coagulation
d_p = particle diameter
$\mathcal{D}$ = "death" rate associated to particle coagulation
D = Brownian diffusion coefficient
Dam = Damköhler number ($Dam \equiv t_V/t_\beta$)
$f(v)$ = particle size distribution function
F = correction factor
m = mass of single particle or gas molecule
M = molecular weight
$n(v)$ = number density of particles with volume v
N = number density of particles
p = pressure
p_{ij} = pair distribution density function
Pe = Peclet number
r = radial coordinate
$\mathcal{R}$ = ideal gas constant
S = speed ratio parameter (Eq. 27)
t = time
t_β = characteristic coagulation time ($t_\beta = (N_0\beta_{ref})^{-1}$)
t_V = characteristic expansion time ($t_V = (Dln\rho^{-1}/Dt)^{-1}$)
T = temperature
v = radial velocity
v = particle volume
x = dimensionless particle volume (v/v_{ref})
Z = compressibility factor ($pV/(\mathcal{R}T)$)

Greek letters and operators

β = coagulation rate constant
β_2 = PSD kurtosis
γ_g = specific heat ratio (c_p/c_V)
γ_1 = PSD skewness
ϕ = suspended particle volume fraction
ρ = mass density
ρ^{-1} = specific volume of the carrier fluid
σ = PSD standard deviation
μ = shear viscosity
D/Dt = material derivative operator
def = deformation rate (differential) operator
div = divergence (differential) operator
erf = error function
erfc = complementary error function (erfc $(x) = 1 - $ erf (x))
erfi = imaginary error function (erfi $(x) = -i$ erf (ix), with $i^2 = -1$)
$\mathcal{O}()$ = order-of-magnitude "operator"

Subscripts and superscripts

0 = at initial time
∞ = far from target particle
eff = "effective" value
fm = free-molecule limit
g = gas
ref = 'reference' value
S = corresponding to carrier vapor ("solvent")
V = corresponding to carrier vapor expansion
w = at target particle surface

Abbreviations/acronyms

BC = boundary condition
CNT = classical nucleation theory

CSD = crystal size distribution
Dam = Damköhler number
DMSO = dimethyl sulfoxide (solvent)
EM = energetic material
EOS = equation of state
GASP = gas antisolvent precipitation
GDE = General dynamic equation[16]
HMX = $C_4H_8O_8N_8$ "octogen": EM
N/G/C = nucleation, growth, and coagulation
PSD = particle size distribution
QS = quasi-steady
RESS = rapid expansion of a supercritical solvent
RDX = $C_3H_6O_6N_6$ "hexogen" (cyclonite): EM
SASP = supercritical antisolvent precipitation
SCF = supercritical fluid
TIP = thermodynamics of irreversible processes

Literature Cited

1. de Groot SR, Mazur P. *Non-Equilibrium Thermodynamics*. Amsterdam: North Holland, 1962; Reprinted 1984, Dover.
2. Haase R. *Thermodynamics of Irreversible Processes*. Boston, MA: Addison-Wesley, 1969; Reprinted 1990, Dover.
3. Rosner DE. *Transport Processes in Chemically Reacting Flow Systems*. Stoneham, MA: Butterworth-Heinemann, 1986; Reprinted 2000, Dover (4th. printing with 48p. appendix/updates; see Ex.3.17, p555).
4. Hirschfelder JO, Curtiss CF, Bird RB. *The Molecular Theory of Gases and Liquids*, 2nd ed. New York, NY: Wiley, 1964 (Corrected with Notes Added to 1st ed., 1954).
5. Bird RB, Stewart WE, Lightfoot EN. *Transport Phenomena*, 2nd ed. New York, NY: Wiley, 2007.
6. Eckert CA, Knutson BL, Dibenedetti PG. Supercritical fluids as solvents for chemical and materials processing. *Nature*. 1996;383:313–318.
7. Schmitt WJ. Finely divided powders by carrier solution injection into a near- or super-critical fluid. *AIChE J*. 1995;41:2476–2486.
8. Kikic I, Sist P. In: Kiran E, Debenedetti PG, Peters CJ, editors. Applications of supercritical fluids to pharmaceuticals: controlled drug release systems. Supercritical Fluids: Fundamentals and Applications, Vol. E366 *of NATO Science Series*. Dordrecht: Kluwer Academic Publishers, 2000:291–306.
9. Lora M, Bertucco A, Kikic I. Simulation of the semi-continuous supercritical anti-solvent recrystallization process. *Ind Eng Chem Res*. 2000;39:1487–1496.
10. Jung J, Perrut M. Particle design using supercritical fluids: literature and patent survey. *J Supercrit Fluids*. 2001;20:179–219.
11. Fages J, Lochard H, Letourneau JJ, Sauceau M, Rodier E. Particle generation for pharmaceutical application using supercritical fluid technology. *Powder Technol*. 2004;141:219–226.
12. Reverchon E, Kröber H, Teipel U. Crystallization with compressed gases. In: Teipel U, editor. *Energetic Materials: Particle Processing and Characterization*. Weinheim: Wiley-VCH, 2005, Chapter 4:159–182.
13. Reverchon E, Adami R, Caputo G, De Marco I. Spherical microparticles production by supercritical anti-solvent precipitation: interpretation of results. *J Supercrit Fluids*. 2008;47:70–84.
14. Chavez F, Dibenedetti PG, Luo JJ, Dave RN, Pfeffer R. Estimation of the characteristic time scales in the supercritical anti-solvent process. *Ind Eng Chem Res*. 2003;42:3156–3162.
15. Zebel G. Coagulation of aerosols. Davies CN, editors. *Aerosol Science*. New York: Academic Press, 1966, Chapter 2:31–58.
16. Friedlander SK. *Smoke, Dust and Haze–Fundamentals of Aerosol Dynamics*, 2nd ed. New York: Oxford University Press, 2000.
17. Mackowski DW, Tassopoulos M, Rosner DE. Effect of radiative heat transfer on the coagulation dynamics of combustion-generated particles. *Aerosol Sci Technol*. 1994;20:83–99.
18. McGraw R. Description of aerosol dynamics by the quadrature method of moments. *Aerosol Sci Technol*. 1997;27:255–265.
19. Wright R, McGraw R, Rosner DE. Bivariate extension of the quadrature method of moments for modeling simultaneous coagulation and sintering of particle populations. *J Colloid Interface Sci*. 2001;236:242–251.
20. Boyd JP. *Chebyshev and Fourier Spectral Methods*, 2nd ed. New York: Dover, 2000.
21. Arias-Zugasti M. Application of orthogonal collocation in aerosol science: fast calculation of the coagulation tensor. *J Aerosol Sci*. 2006;37:1356–1369.
22. Vemury S, Pratsinis SE. Self-preserving size distributions of agglomerates. *J Aerosol Sci*. 1995;26:175–185.
23. Noyes RM. Effect of diffusion rates on chemical kinetics. *Prog React Kinet*. 1961;1:129–160.
24. Wilemski G, Fixman M. General theory of diffusion-controlled reactions. *J Chem Phys*. 1973;58:4009–4019.
25. Rice SA. *Diffusion-limited reactions. Comprehensive Chemical Kinetics*, *Vol*. 25. In: Bamford CH, Tipper CFH, Compton RG, editors. Amsterdam: Elsevier, 1985.
26. Szabo A. Theory of diffusion-influenced fluorescence quenching. *J Phys Chem*. 1989;93:6929–6939.
27. Xing Y, Rosner DE, Köylü UO, Tandon P. Morphological evolution of oxide nano-particles in laminar counterflow diffusion flames; measurements and modeling. *AIChE J*. 1997;43:2641–2649; Invited Paper for AIChE J (special issue on: Ceramics Processing).
28. Rosner DE, Park HM. Thermophoretically augmented mass-, momentum- and energy-transfer rates in high particle mass loaded laminar forced convection systems (see Appendix 5; add missing exponent − 1 to far RHS of Eq. (A5–1)). *Chem Eng Sci*. 1988;43:2689–2704.
29. Reguera D, Rubí JM. Homogeneous nucleation in inhomogeneous media. I. Nucleation in a temperature gradient. *J Chem Phys*. 2003; 119:9877–9887.
30. Reguera D, Rubí JM. Homogeneous nucleation in inhomogeneous media. II. Nucleation in a shear flow. *J Chem Phys*. 2003;119:9888–9893.
31. Katz JL. Condensation of a supersaturated vapor. 1. Homogeneous nucleation of normal-alkanes. *J Chem Phys*. 1970;52:4733–4748.
32. Belfiori LA, Karim MN, Belfiori CJ. Tubular bioreactor models that include Onsager-Curie scalar cross-phenomena to describe stress-dependent rates of cell proliferation. *Biophys Chem*. 2008;135:41–50.
33. Belfiore LA, Bonani W, Leoni M, Belfiore CJ. Stress-sensitive nutrient consumption via steady and non-reversing dynamic shear in continuous-flow rotational bioreactors. *Biophys Chem*. 2009;141:140–152.
34. Patterson GN. *Molecular Flow of Gases*. New York: Wiley, 1956.
35. Turner JR, Kodas TT, Friedlander SK. Monodisperse particle production by vapor condensation in nozzles. *J Chem Phys*. 1988;88:457–465.
36. Tom J, Debenedetti PG. Particle formation with supercritical fluid-semdash]a review. *J Aerosol Sci*. 1991;22:555–584.
37. Kwauk X, Debenedetti PG. Mathematical modeling of aerosol formation by rapid expansion of supercritical solutions in a converging nozzle. *J Aerosol Sci*. 1993;24:445–469.
38. Shaub GR, Brennecke JF, McCready MJ. Radial model for particle formation from the rapid expansion of supercritical solutions. *J Supercrit Fluids*. 1995;8:318–328.
39. Reverchon E, Pallado P. Hydrodynamic modeling of the RESS process. *J Supercrit Fluids*. 1996;9:216–221.
40. Turk M. Formation of small organic particles by RESS: experimental and theoretical investigations. *J Supercrit Fluids*. 1999;15:79–89.
41. Turk M. Influence of thermodynamic behaviour and solute properties on homogenerous nucleation in supercritical solutions. *J Supercrit Fluids*. 2000;18:169–184.
42. Fernandez de la Mora J, Mercer J, Rosner DE, Fenn JB. Simplified kinetic treatment of heavy molecule velocity persistence effects: application to species separation. In: Fisher SS, editor. *Progress in Astronautics and Aeronautics*, *Vol*. 74: *Rarefied Gas Dynamics Paper 186 of 12th* AIAA: New York, 1981:617–626 *International Symposium on Rarefied Gas Dynamics*.

Manuscript received Aug. 11, 2009, and revision received Mar. 29, 2010.